Implications of fermionic dark matter on recent neutrino oscillation data *

Shivaramakrishna Singirala

School of Physics, University of Hyderabad, Hyderabad - 500046, India

Abstract: We investigate flavor phenomenology and dark matter in the context of the scotogenic model. In this model, the neutrino masses are generated through radiative corrections at the one-loop level. Considering the neutrino mixing matrix to be of tri-bimaximal form with additional perturbations to accommodate the recently observed non-zero value of the reactor mixing angle θ_{13}, we obtain the relation between various neutrino oscillation parameters and the model parameters. Working in a degenerate heavy neutrino mass spectrum, we obtain light neutrino masses obeying the normal hierarchy and also study the relic abundance of fermionic dark matter candidates, including coannihilation effects. A viable parameter space is thus obtained, consistent with neutrino oscillation data, relic abundance and various lepton flavor violating decays such as $l_\alpha \to l_\beta \gamma$ and $l_\alpha \to 3l_\beta$.

Keywords: dark matter, neutrino mixing, lepton flavor violation.

PACS: 13.35.−r, 14.60.Pq, 95.35.+d **DOI:** 10.1088/1674-1137/41/4/043102

1 Introduction

The Standard Model (SM) of particle physics has been very successful in explaining physics at the fundamental level. However, there are still many open questions for which it does not provide any satisfactory answer. The existence of dark matter (DM) and the observation of non-zero neutrino masses stand as some of the few robust pieces of evidence for physics beyond the SM.

Considerable progress has been made in the determination of neutrino mass squared differences and mixing parameters from the data of various solar and atmospheric neutrino oscillation experiments. Theoretically, the smallness of neutrino mass can be generally explained by the well known seesaw mechanisms, namely: type-I [1], type-II [2], type-III [3] and radiative seesaw [4]. In standard parametrization, the mechanism of mixing can be described by the unitary Pontecorvo-Maki-Nakagawa-Sakata (PMNS) matrix $V_{\rm PMNS}$ [5] written in terms of three rotation angles θ_{12}, θ_{23}, θ_{13} and three CP-violating phases namely δ_{CP} (Dirac type) and ρ,σ (Majorana type) as

$$V_{\rm PMNS} \equiv U_{\rm PMNS} \cdot P_\nu = \begin{pmatrix} c_{12}c_{13} & s_{12}c_{13} & s_{13}e^{-i\delta_{CP}} \\ -s_{12}c_{23} - c_{12}s_{13}s_{23}e^{i\delta_{CP}} & c_{12}c_{23} - s_{12}s_{13}s_{23}e^{i\delta_{CP}} & c_{13}s_{23} \\ s_{12}s_{23} - c_{12}s_{13}c_{23}e^{i\delta_{CP}} & -c_{12}s_{23} - s_{12}s_{13}c_{23}e^{i\delta_{CP}} & c_{13}c_{23} \end{pmatrix} P_\nu \,, \quad (1)$$

where $c_{ij} \equiv \cos\theta_{ij}$, $s_{ij} \equiv \sin\theta_{ij}$ and $P_\nu \equiv \{e^{i\rho}, e^{i\sigma}, 1\}$ is a diagonal phase matrix. The mixing angles as well as the mass squared differences have been well constrained by various neutrino oscillation experiments. Recently, the Daya Bay [6, 7], RENO [8] and T2K [9] collaborations have precisely measured the reactor mixing angle θ_{13} with a moderately large value. However, there are several missing pieces such as the neutrino mass hierarchy, the magnitude of the CP violating phase δ_{CP}, the absolute scale of the neutrino mass, and the nature of neutrinos (whether Dirac or Majorana). Various neutrino oscillation parameters derived from a global analysis of recent oscillation data taken from Ref. [10] are presented in Table 1.

Turning to dark matter, its particle nature is still a mystery. The recent survey by PLANCK [11] reveal that DM constitutes about 26.8% of the total energy budget of the Universe. Various cosmological observations suggest that this unknown particle is non-relativistic in nature and is stable on cosmological time scales. Numerous beyond-SM scenarios study DM phenomenology by imposing additional discrete symmetry such as R-parity, Z_2 symmetry etc. Weakly Interacting Massive Particles (WIMPs) are the best motivated DM candidate. They

Received 14 July 2016, Revised 23 November 2016

∗ I would like to thank Rukmani Mohanta for helpful suggestions. This work is supported by DST-Inspire Fellowship division - IF130927

are massive particles with cross sections of approximately the order of the weak interaction cross section.

Table 1. Best-fit values with their 3σ ranges of the neutrino oscillation parameters from Ref. [10] where NO indicates normal ordering.

mixing parameters	best fit value	3σ range
$\sin^2\theta_{12}$	0.323	$0.278 \to 0.375$
$\sin^2\theta_{23}$ (NO)	0.567	$0.392 \to 0.643$
$\sin^2\theta_{13}$ (NO)	0.0234	$0.0177 \to 0.0294$
δ_{CP} (NO)	1.34π	$(0 \to 2\pi)$
$\Delta m^2_{31}/10^{-3}$ eV^2 (NO)	2.48	$2.3 \to 2.65$
$\Delta m^2_{21}/10^{-5}$ eV^2	7.60	$7.11 \to 8.18$

It would be interesting to study extensions of the Standard Model that can relate these two issues. The scotogenic model proposed by Ma [4] is one such framework in which neutrino mass generation involves interaction with dark matter. In this model an unbroken discrete symmetry forbids neutrinos attaining a tree level mass and also assures the stability of DM particles. It is a suitable platform to simultaneously explain neutrino oscillation data and DM phenomenology.

In this work, we consider the scotogenic model to correlate some of the neutrino oscillation parameters, like the mass squared differences and the mixing angles with the model parameters. We examine the neutrino radiative mass matrix using the mixing matrix of TBM type with added perturbation to achieve large θ_{13}. We solve for suitable flavor structure to study neutrino phenomenology. We then use the best fit values on neutrino oscillation parameters to constrain the parameter space of this model. In addition, we study DM relic abundance choosing the lightest odd particle as the DM candidate. We scan over the entire parameter space of the model imposing the constraints from neutrino data, DM observables and lepton flavor violating decays.

The paper is organized as follows. In Section 2 we describe the scotogenic model. In Section 3 we diagonalize the neutrino radiative mass matrix and obtain solutions to explain neutrino oscillation data. The fermionic DM relic abundance considering the coannihilation effects is studied in Section 4 and then in Section 5 we estimate the branching ratios of various LFV decays. We conclude our discussion in Section 6.

2 Scotogenic model

The scotogenic model is a minimal extension of the SM with an additional inert scalar doublet η and three heavy Majorana right-handed neutrinos N_i $(i = 1,2,3)$. The potential is imposed with a discrete symmetry under which all the new particles i.e., N_i and η, are odd, and SM particles are even. The unbroken discrete symmetry guarantees the coupling of the inert doublet to fermions vanish and doesn't get a vacuum expectation value (VEV), while the SM Higgs doublet ϕ obtains a VEV $\langle\phi^0\rangle = v$ by the spontaneous symmetry breaking of $SU(2)_L \times U(1)_Y$ global symmetry. This model is rich in phenomenology providing scalar and fermionic dark matter candidates. Scalar dark matter in this model has been studied extensively in the literature [12–14].

The scalar potential of this model is given by [15]

$$\begin{aligned} V = {} & m_\phi^2\phi^\dagger\phi + m_\eta^2\eta^\dagger\eta + \frac{1}{2}\lambda_1(\phi^\dagger\phi)^2 \\ & + \frac{1}{2}\lambda_2(\eta^\dagger\eta)^2 + \lambda_3(\phi^\dagger\phi)(\eta^\dagger\eta) \\ & + \lambda_4(\phi^\dagger\eta)(\eta^\dagger\phi) + \frac{1}{2}\lambda_5[(\phi^\dagger\eta)^2 + (\eta^\dagger\phi)^2], \end{aligned} \tag{2}$$

where the two scalar doublets ϕ and η are defined as

$$\phi = \begin{pmatrix} \phi^+ \\ \phi^0 \end{pmatrix}, \qquad \eta = \begin{pmatrix} \eta^+ \\ \eta^0 \end{pmatrix}. \tag{3}$$

After spontaneous symmetry breaking, the masses of the charged component (η^+) and neutral components of $\eta^0 = (\eta_R + \mathrm{i}\eta_I)/\sqrt{2}$ are given by

$$\begin{aligned} m^2_{\eta^+} &= m^2_\eta + \lambda_3 v^2, \\ m^2_R &= m^2_\eta + (\lambda_3 + \lambda_4 + \lambda_5)v^2, \\ m^2_I &= m^2_\eta + (\lambda_3 + \lambda_4 - \lambda_5)v^2. \end{aligned} \tag{4}$$

The Yukawa Lagrangian of this model is [15]

$$\begin{aligned} \mathcal{L}_N = {} & \overline{N_i}\mathrm{i}\partial\!\!\!/ P_R N_i + (D_\mu\eta)^\dagger(D^\mu\eta) \\ & - \frac{M_i}{2}\overline{N_i{}^c}P_R N_i + h_{\alpha i}\overline{\ell_\alpha}\eta^\dagger P_R N_i + \text{h.c.}, \end{aligned} \tag{5}$$

where $h_{\alpha i}$ are the Yukawa couplings, α denotes the lepton flavor and M_i are the masses of heavy neutrinos N_i.

In this model, neutrinos get their mass by a loop correction called the "radiative seesaw mechanism". The corresponding neutrino mass matrix is given by

$$(\mathcal{M}_\nu)_{\alpha\beta} = \sum_{i=1}^{3} h_{\alpha i}h_{\beta i}\Lambda_i, \tag{6}$$

where Λ_i is defined as

$$\Lambda_i = \frac{\lambda_5 v^2}{8\pi^2 M_i} I(r_i), \quad I(x) = \frac{x^2}{1-x^2}\left(1 + \frac{x^2}{1-x^2}\ln x^2\right), \tag{7}$$

Here the parameters r_i are defined as $r_i = M_i/m_0$ and ${m_0}^2 = ({m_R}^2 + {m_I}^2)/2$. We take $\lambda_5 \sim 10^{-10}$, a very small value, in order to have correct neutrino masses and also probe for lepton flavor violation [15–18]. We now diagonalize the radiative mass matrix (6) using the PMNS matrix to explain neutrino oscillation data.

3 Neutrino phenomenology

Various neutrino experiments have confirmed that neutrinos have tiny mass and that they oscillate from one flavor to another as they propagate. The phenomenon of neutrino oscillation is described by solar (θ_{12}), atmospheric (θ_{23}) and reactor (θ_{13}) mixing angles. Of these three rotation angles, two are large (θ_{12} and θ_{23}), and one is not so large (θ_{13}). Originally, it was believed that the reactor mixing angle would be very small and with this motivation numerous models were proposed which are generally based on some discrete flavor symmetries such as S_3, S_4, A_4, etc [19] to explain the neutrino mixing pattern. For instance, the tri-bimaximal (TBM) mixing pattern [20], a well motivated model which has $\sin^2\theta_{12}=\frac{1}{3}$ and $\sin^2\theta_{23}=\frac{1}{2}$ and which can be expressed in a generalized form as

$$U_\nu^0=\begin{pmatrix} \cos\theta & \sin\theta & 0 \\ -\frac{\sin\theta}{\sqrt{2}} & \frac{\cos\theta}{\sqrt{2}} & \frac{1}{\sqrt{2}} \\ \frac{\sin\theta}{\sqrt{2}} & -\frac{\cos\theta}{\sqrt{2}} & \frac{1}{\sqrt{2}} \end{pmatrix}, \tag{8}$$

with $\theta\simeq 35^\circ$. However, in the TBM mixing pattern the value of θ_{13} turns out to be zero. After the experimental evidence of a moderately large θ_{13}, it was found that by adding suitable perturbation terms, the TBM mixing pattern can still describe the neutrino mixing pattern with sizeable θ_{13}. As discussed in Ref. [21], here we consider a simple perturbation matrix, i.e., a rotation matrix in the 13 plane, which can provide the required corrections to the various mixing angles of the TBM mixing matrix. Assuming the charged lepton mass matrix is diagonal (i.e., the identity matrix), one can write the PMNS mixing matrix, which relates the flavor eigenstates to the corresponding mass eigenstates, as

$$U_{\rm PMNS}=U_\nu^0\begin{pmatrix} \cos\varphi & 0 & {\rm e}^{-{\rm i}\zeta}\sin\varphi \\ 0 & 1 & 0 \\ -{\rm e}^{{\rm i}\zeta}\sin\varphi & 0 & \cos\varphi \end{pmatrix}. \tag{9}$$

In our work, we consider the phase ζ to be zero for convenience. Now we diagonalize the mass matrix (6) by the mixing matrix (9) using the relation $U_{\rm PMNS}^{\rm T}\mathcal{M}_\nu U_{\rm PMNS}={\rm diag}(m_1,m_2,m_3)$. This in turn provides the following conditions (vanishing off-diagonal elements of the mass matrix) to be satisfied:

$$\begin{aligned}
&\sum_{i=1}^{3}\frac{h_{ei}^2}{2}\sin 2\theta\cos\varphi+\frac{h_{ei}(h_{\mu i}-h_{\tau i})}{\sqrt{2}}\cos 2\theta\cos\varphi\\
&-\frac{(h_{\mu i}-h_{\tau i})^2}{4}\sin 2\theta\cos\varphi\\
&-\frac{h_{ei}(h_{\mu i}+h_{\tau i})}{\sqrt{2}}\sin\theta\sin\varphi\\
&-\frac{(h_{\mu i}^2-h_{\tau i}^2)}{2}\cos\theta\sin\varphi=0,
\end{aligned} \tag{10a}$$

$$\begin{aligned}
&\sum_{i=1}^{3}\frac{h_{ei}^2}{2}\sin 2\theta\sin\varphi+\frac{h_{ei}(h_{\mu i}-h_{\tau i})}{\sqrt{2}}\cos 2\theta\sin\varphi\\
&-\frac{(h_{\mu i}-h_{\tau i})^2}{4}\sin 2\theta\sin\varphi\\
&+\frac{h_{ei}(h_{\mu i}+h_{\tau i})}{\sqrt{2}}\sin\theta\cos\varphi\\
&+\frac{(h_{\mu i}^2-h_{\tau i}^2)}{2}\cos\theta\cos\varphi=0,
\end{aligned} \tag{10b}$$

$$\begin{aligned}
&\sum_{i=1}^{3}\frac{h_{ei}^2}{2}\cos^2\theta\sin 2\varphi-\frac{h_{ei}(h_{\mu i}-h_{\tau i})}{2\sqrt{2}}\sin 2\theta\sin 2\varphi\\
&+\frac{(h_{\mu i}-h_{\tau i})^2}{4}\sin^2\theta\sin 2\varphi\\
&+\frac{h_{ei}(h_{\mu i}+h_{\tau i})}{\sqrt{2}}\cos\theta\cos 2\varphi-\frac{(h_{\mu i}^2-h_{\tau i}^2)}{2}\sin\theta\cos 2\varphi\\
&-\frac{(h_{\mu i}+h_{\tau i})^2}{4}\sin 2\varphi=0.
\end{aligned} \tag{10c}$$

The neutrino mass eigenvalues are given by

$$\begin{aligned}
m_1=&\sum_{i=1}^{3}\Big(h_{ei}^2\cos^2\theta\cos^2\varphi-\frac{1}{\sqrt{2}}h_{ei}(h_{\mu i}-h_{\tau i})\sin 2\theta\cos^2\varphi\\
&-\frac{1}{\sqrt{2}}h_{ei}(h_{\mu i}+h_{\tau i})\cos\theta\sin 2\varphi\\
&+\frac{1}{2}(h_{\mu i}+h_{\tau i})^2\sin^2\varphi+\frac{1}{2}(h_{\mu i}^2-h_{\tau i}^2)\sin\theta\sin 2\varphi\\
&+\frac{1}{2}(h_{\mu i}-h_{\tau i})^2\sin^2\theta\cos^2\varphi\Big)\Lambda_i\,,\\
m_2=&\sum_{i=1}^{3}\Big(h_{ei}^2\sin^2\theta+\frac{1}{\sqrt{2}}h_{ei}(h_{\mu i}-h_{\tau i})\sin 2\theta\\
&+\frac{1}{2}(h_{\mu i}-h_{\tau i})^2\cos^2\theta\Big)\Lambda_i\,,\\
m_3=&\sum_{i=1}^{3}\Big(h_{ei}^2\cos^2\theta\sin^2\varphi-\frac{1}{\sqrt{2}}h_{ei}(h_{\mu i}-h_{\tau i})\sin 2\theta\sin^2\varphi\\
&+\frac{1}{\sqrt{2}}h_{ei}(h_{\mu i}+h_{\tau i})\cos\theta\sin 2\varphi\\
&+\frac{1}{2}(h_{\mu i}+h_{\tau i})^2\cos^2\varphi-\frac{1}{2}(h_{\mu i}^2-h_{\tau i}^2)\sin\theta\sin 2\varphi\\
&+\frac{1}{2}(h_{\mu i}-h_{\tau i})^2\sin^2\theta\sin^2\varphi\Big)\Lambda_i\,.
\end{aligned} \tag{11}$$

Solving (10a), (10b) and substituting in (10c), we obtain two solutions given by

$$1)\qquad h_{\mu i_1}\neq -h_{\tau i_1},\quad \tan\theta=\frac{(h_{\tau i_1}-h_{\mu i_1})}{\sqrt{2}h_{ei_1}},$$
$$\tan 2\varphi=\frac{-\left(\frac{h_{ei_1}(h_{\mu i_1}+h_{\tau i_1})}{\sqrt{2}}\cos\theta-\frac{(h^2_{\mu i_1}-h^2_{\tau i_1})}{2}\sin\theta\right)}{\left(\frac{h^2_{ei_1}}{2}\cos^2\theta-\frac{h_{ei_1}(h_{\mu i_1}-h_{\tau i_1})}{2\sqrt{2}}\sin 2\theta+\frac{(h_{\mu i_1}-h_{\tau i_1})^2}{4}\sin^2\theta-\frac{(h_{\mu i_1}+h_{\tau i_1})^2}{4}\right)},$$

$$2)\qquad h_{\mu i_2}=-h_{\tau i_2},\quad \tan\theta=\frac{h_{ei_2}}{\sqrt{2}h_{\mu i_2}}, \tag{12}$$

where i_1, i_2 can take any value of $i(=1,2,3)$. As shown in Ref. [21], the above mixing matrix can explain recent neutrino oscillation data with the unperturbed mixing as TBM type (i.e., with $\theta=35^\circ$) and the perturbed angle $\varphi=12^\circ$, which accommodates the experimentally measured mixing angles. Thus, Eq. (12) gets further simplified to three simple solutions and the obtained flavor structure, written in terms of $h_{ei}(=h_i)$ in a matrix labelled with the lepton flavor α as row index and $i=1,2,3$ as column index, is given by

$$h_{\alpha i}=\begin{pmatrix} h_1 & h_2 & h_3 \\ -0.68\ h_1 & h_2 & 3.56\ h_3 \\ 0.31\ h_1 & -h_2 & 4.55\ h_3 \end{pmatrix}. \tag{13}$$

Here $i_1=1,3$ and $i_2=2$ is assumed so that the mass eigenvalues (11) get non-zero contributions given as

$$\begin{aligned} m_1&=c_1(h_1^2\Lambda_1),\\ m_2&=c_2(h_2^2\Lambda_2),\\ m_3&=c_3(h_3^2\Lambda_3), \end{aligned} \tag{14}$$

where the coefficients $c_1=1.55$, $c_2=3.04$, $c_3=34.44$. Thus, the flavor structure (13) is suitable to explain normal hierarchy i.e., $(m_3\gg m_2>m_1)$ provided we assume that N_1 and N_2 are degenerate. Imposing the best fit values given in Table 1, the constraints from neutrino mass squared differences are given by

$$\begin{aligned} &[(c_2h_2^2)^2-(c_1h_1^2)^2]\Lambda_1^2=7.6\times10^{-5}\ \text{eV}^2,\\ &[(c_3h_3^2\Lambda_3)^2-(c_2h_2^2\Lambda_1)^2]=2.4\times10^{-3}\ \text{eV}^2. \end{aligned} \tag{15}$$

Thus, we have a free parameter space spanned by $h_i, r_{1,3}$ and $M_{1,3}$. We now proceed to constrain the parameter space with the DM relic abundance, choosing the lightest of the odd particles as a DM candidate.

4 Relic abundance

We choose N_1 as the lightest odd particle and since N_2 is its degenerate partner, the relic abundance gets contributions from annihilation as well as coannihilation channels. To include the coannihilation effects, we adopt the procedure given in Ref. [22] in the estimation of relic abundance. We introduce a parameter δ given by $\delta\equiv(M_2-M_1)/M_1$, which depicts the mass splitting ratio of the degenerate neutrinos. The effective cross section σ_{eff}, including contributions from coannihilations, is given by

$$\begin{aligned} \sigma_{\text{eff}}&=\frac{g^2_{N_1}}{g^2_{\text{eff}}}\sigma_{N_1N_1}+2\frac{g_{N_1}g_{N_2}}{g^2_{\text{eff}}}\sigma_{N_1N_2}(1+\delta)^{3/2}\text{e}^{-\delta x}\\ &\quad+\frac{g^2_{N_2}}{g^2_{\text{eff}}}\sigma_{N_2N_2}(1+\delta)^3\text{e}^{-2\delta x},\\ g_{\text{eff}}&=g_{N_1}+g_{N_2}(1+\delta)^{3/2}\text{e}^{-\delta x}. \end{aligned} \tag{16}$$

Here g_{eff} denotes the effective degrees of freedom, $g_{N_{1,2}}$ are the number of degrees of freedom for Majorana fermions and $x=M_1/T$, where T is the temperature. The (co)annihilation cross section of N_i and N_j is given by [15]

$$\begin{aligned} \sigma_{N_iN_j}|v_{\text{rel}}|&=\frac{1}{8\pi}\frac{M_1^2}{(M_1^2+m_0^2)^2}\left[1+\frac{m_0^4-3m_0^2M_1^2-M_1^4}{3(M_1^2+m_0^2)^2}v^2_{\text{rel}}\right]\\ &\quad\times\sum_{\alpha,\beta}(h_{\alpha i}h_{\beta j}-h_{\alpha j}h_{\beta i})^2\\ &\quad+\frac{1}{12\pi}\frac{M_1^2(M_1^4+m_0^4)}{(M_1^2+m_0^2)^4}v^2_{\text{rel}}\\ &\quad\sum_{\alpha,\beta}h_{\alpha i}h_{\alpha j}h_{\beta i}h_{\beta j}. \end{aligned} \tag{17}$$

In the above expression i,j can be 1 or 2 and v_{rel} represents the relative velocity of annihilating particles. The effective annihilation cross section is defined as $\sigma_{\text{eff}}|v_{\text{rel}}|=a_{\text{eff}}+b_{\text{eff}}v^2_{\text{rel}}$. The coefficients a_{eff} and b_{eff} for the obtained flavor structure (13) are given by

$$a_{\text{eff}}=\frac{1}{16\pi}\frac{M_1^2}{(M_1^2+m_0^2)^2}(s_{12}h_1^2h_2^2), \tag{18}$$

$$\begin{aligned} b_{\text{eff}}&=\frac{1}{48\pi}\frac{M_1^2(M_1^4+m_0^4)}{(M_1^2+m_0^2)^4}[(s_1h_1^4+s_2h_2^4)]\\ &\quad+\frac{1}{16\pi}\frac{M_1^2}{(M_1^2+m_0^2)^2}\left[\frac{m_0^4-3m_0^2M_1^2-M_1^4}{3(M_1^2+m_0^2)^2}\right](s_{12}\ h_1^2h_2^2), \end{aligned} \tag{19}$$

where $s_1 = 2.42, s_2 = 9.24$ and $s_{12} = 9.47$. Now the thermally averaged cross section is given as $\langle\sigma_{\rm eff}|v_{\rm rel}|\rangle = a_{\rm eff} + 6b_{\rm eff}/x$. If the decoupling temperature is given by $T_f = M_1/x_f$, the relic abundance can be estimated by

$$\Omega_{N_1}h^2 = \frac{1.07\times10^9\ {\rm GeV}^{-1}}{g_\star^{1/2}m_{\rm pl}}\frac{1}{J(x_f)}, \tag{20}$$

where $m_{\rm pl} = 1.22\times10^{19}$ GeV and $g_\star = 106.75$ and $J(x_f)$ is given by

$$J(x_f) = \int_{x_f}^{\infty}\frac{\langle\sigma_{\rm eff}|v_{\rm rel}|\rangle_{\rm eff}}{x^2}\ {\rm d}x. \tag{21}$$

Using the first relation in Eq. (15), we eliminate h_2 and since N_1 is the lightest odd particle, we take $r_1 < 1$ [15, 18] and $|h_i| < 1.5$ [16]. Figure 1 depicts the allowed parameter space (h_1, r_1) consistent with current bounds on relic abundance [11]. Figure 2 displays the relic abundance as a function of DM mass for various values of h_1 at two representative values of r_1, i.e., $r_1 = 0.5$ in the left panel and $r_1 = 0.6$ in the right panel. This shows that the mass range of DM mass consistent with current relic abundance is proportional with the parameter r_1 and the Yukawa coupling h_1.

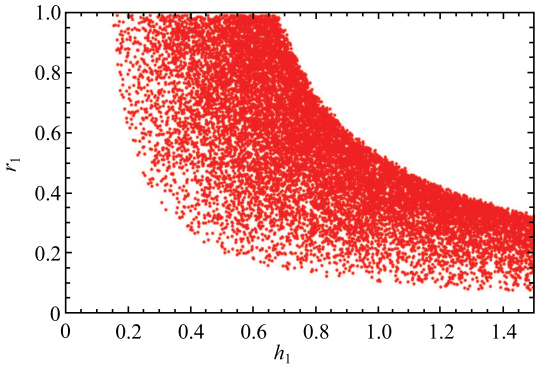

Fig. 1. Parameter space of h_1 and r_1 consistent with 3σ relic abundance.

As the light neutrinos oscillate in flavor, one-loop diagrams contribute to lepton flavor violating decays. We now further constrain the parameter space of the model using these decays.

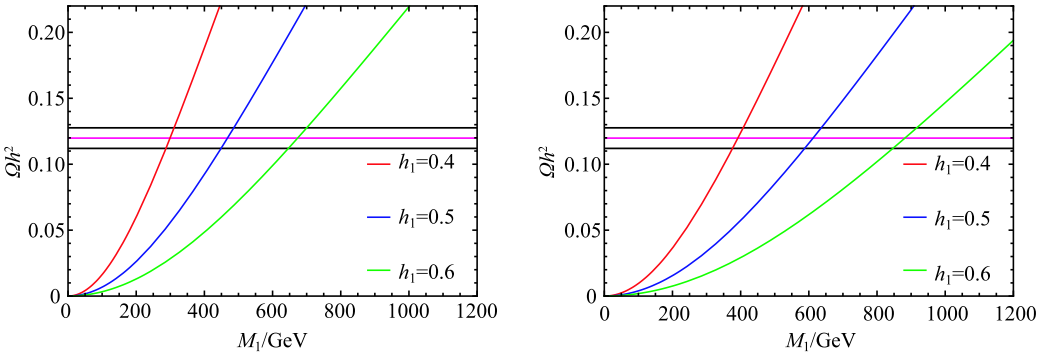

Fig. 2. (color online) Variation of relic abundance with DM mass for various values of h_1 at $r_1 = 0.5$ (left panel) and $r_1 = 0.6$ (right panel) where the horizontal line (magenta) represents the central value of the relic density and the black lines denote their corresponding 3σ range.

5 Lepton flavour violating decays

The observation of neutrino oscillations has provided an unambiguous signal for lepton number violation in the neutral lepton sector, even though individual lepton number is conserved in electroweak interactions in the SM. The evidence of light neutrino masses and mixing and the violation of family lepton number could in principle allow flavor changing neutral current (FCNC) transitions in the charged lepton sector as well, such as $l_\alpha \to l_\beta\gamma$ and $l_\alpha \to l_\beta\overline{l}_\beta l_\beta$.

The expression for the branching ratio of lepton flavor violating decay process $l_\alpha \to l_\beta\gamma$ written in terms of dipole form factor A_D is given by [17]

$$Br(l_\alpha \to l_\beta\gamma) = \frac{3(4\pi)^3\alpha_{\rm em}}{4G_F^2}|A_D|^2 Br(l_\alpha \to l_\beta\nu_\alpha\overline{\nu}_\beta), \tag{22}$$

where $\alpha_{\rm em} = e^2/4\pi$ is the electromagnetic fine structure constant, G_F is the Fermi constant and $\alpha(\beta)$ represents the lepton flavor. The diagrams contributing to A_D are shown in Fig. 3 and the expression is given by

$$A_D = \sum_{i=1}^{3}\frac{h^*_{i\beta}h_{i\alpha}}{2(4\pi)^2}\frac{1}{m_0^2}F_2(r_i). \tag{23}$$

Here the expression for the loop function $F_2(x)$ is given in Appendix A and for simplicity we consider $\lambda_4 \ll \lambda_3$, thus we get η^+ and η^0 to be degenerate [15]. Applying the flavour structure (13), the relation (22) becomes

$$Br(\mu\to e\gamma) = \frac{3\alpha_{\rm em}}{64\pi G_F^2 m_0^4}|(h_2^2 - 0.68h_1^2)F_2(r_1) + (3.56h_3^2)F_2(r_3)|^2. \tag{24}$$

We consider $r_3 > 1$, $M_1 < 2$ TeV and $M_3, m_0 < 8$ TeV and thus we work in the mass regime $M_1 \simeq M_2 < m_0 < M_3$. Of all the lepton flavor violating (LFV) decays, the decay channel $\mu \to e\gamma$ provides the most stringent constraint on the parameter space of this model.

Imposing the constraints from neutrino mass squared differences, relic abundance and current upper bounds on $Br(\mu \to e\gamma)$ [23], Fig. 4 (left panel) shows the allowed region in the (h_3, r_3) parameter space of the model. From the figure, the lower bound on r_3 is 2 (i.e., $r_3 > 2$) and the upper bound on h_3 is 0.33 (i.e., $h_3 < 0.33$). Figure 4 (right panel) depicts the variation of h_1 with the mass of DM. It shows that $Br(\mu \to e\gamma)$ excludes the values above 1.2 for h_1. Now taking all the constraints from the flavor and dark sector, one can tabulate the allowed parameter space shown in Table 2.

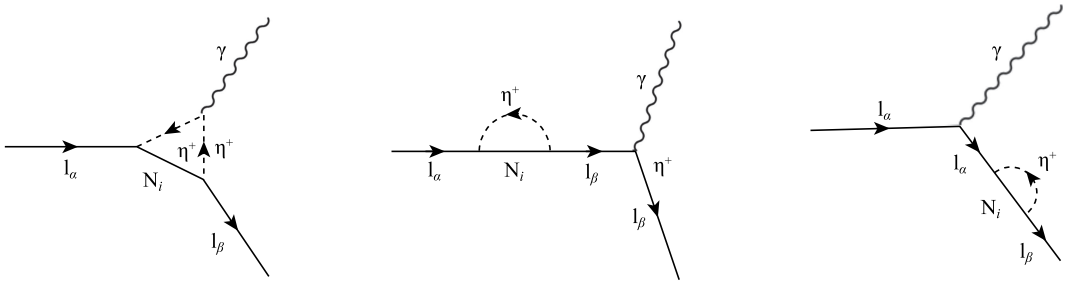

Fig. 3. Diagrams contributing to $l_\alpha \to l_\beta \gamma$.

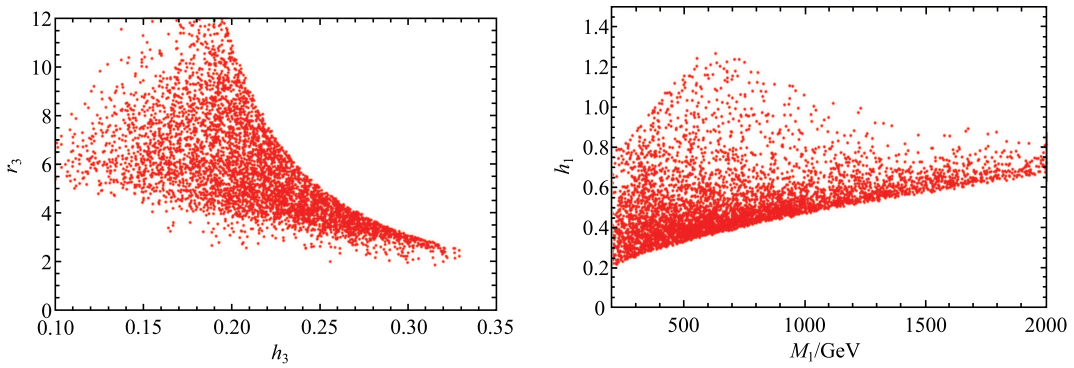

Fig. 4. Parameter space of h_3 and r_3 (left panel) and variation of h_1 with M_1 (right panel) consistent with neutrino oscillation data, relic density and $Br(\mu \to e\gamma)$.

Table 2. Scotogenic model parameters with their range.

parameters	range
r_1	$0.2 \to 1$
r_3	$2 \to 12$
$\|h_1\|$	$0.2 \to 1.2$
$\|h_2\|$	$0.2 \to 1.0$
$\|h_3\|$	$0.1 \to 0.33$

We follow a similar procedure to compute the branching ratios of $\tau \to e\gamma$ and $\tau \to \mu\gamma$ decays. Using the allowed parameter space given in Table 2, we show in Fig. 5 the correlation plot between $Br(\tau \to e\gamma)$ and $Br(\tau \to \mu\gamma)$. In our analysis, we have used the measured branching ratios for $\mu \to \nu_\mu e \bar{\nu}_e$, $\tau^- \to \nu_\tau \mu^- \bar{\nu}_\mu$ and $\tau^- \to \nu_\tau e^- \bar{\nu}_e$ processes from Ref. [23] as

$$\begin{aligned} &Br(\mu \to \nu_\mu e \bar{\nu}_e) = 100\%\,, \\ &Br(\tau \to \nu_\tau \mu \bar{\nu}_\mu) = (17.41 \pm 0.04)\%\,, \\ &Br(\tau \to \nu_\tau e \bar{\nu}_e) = (17.83 \pm 0.04)\%\,. \end{aligned} \tag{25}$$

Now we study lepton flavor violation in 3-body decays. As discussed in Ref. [17], these decays get contributions from three types of loop diagrams, namely : γ-penguin, Z-penguin and box diagrams. The branching ratio for $l_\alpha \to 3 l_\beta$ in the scotogenic model is given by [17]

$$\begin{aligned} &Br\left(l_\alpha \to l_\beta \overline{l_\beta} l_\beta\right) \\ &= \frac{3(4\pi)^2 \alpha_{\rm em}^2}{8 G_F^2} \left[|A_{ND}|^2 + |A_D|^2 \left(\frac{16}{3} \log\left(\frac{m_\alpha}{m_\beta}\right) - \frac{22}{3} \right) \right. \\ &\left. + \frac{1}{6}|B|^2 + \left(-2 A_{ND} A_D^* + \frac{1}{3} A_{ND} B^* - \frac{2}{3} A_D B^* + \text{h.c.} \right) \right] \\ &\times Br\left(l_\alpha \to l_\beta \nu_\alpha \overline{\nu_\beta}\right)\,. \end{aligned} \tag{26}$$

The coefficient A_D denotes the photon dipole contributions given in Eq. (23), while the coefficient A_{ND} represents the form factor with the photonic non-dipole contributions given by

$$A_{ND} = \sum_{i=1}^{3} \frac{h^*_{i\beta} h_{i\alpha}}{6(4\pi)^2} \frac{1}{m_0^2} G_2(r_i). \quad (27)$$

Here $G_2(x)$ is a loop function, which is given in Appendix A. The Z-penguin diagrams shown in Fig. 6 give a negligible contribution to the decay width, as explained in Refs. [17, 18]. Apart from photon dipole and non-dipole penguin contributions, the box diagrams shown in Fig. 7 also contribute to the decay width given by

$$B = \frac{1}{(4\pi)^2 e^2 m_0^2} \sum_{i,j=1}^{3} \left[\frac{1}{2} D_1(r_i, r_j) h^*_{j\beta} h_{j\beta} h^*_{i\beta} h_{i\alpha} + r_i r_j D_2(r_i, r_j)) h^*_{j\beta} h^*_{j\beta} h_{i\beta} h_{i\alpha} \right]. \quad (28)$$

The loop functions $D_1(x,y)$ and $D_2(x,y)$ are provided in Appendix A.

Using the allowed parameter space from Table 2, we show in Fig. 8 the correlation plot between $\mu \to e\gamma$ and $\mu \to eee$ (left panel). Similarly, the right panel in Fig. 8 depicts the correlation plot between branching ratios of $\tau \to eee$ and $\tau \to \mu\mu\mu$. From these figures we conclude that all the obtained branching ratios in the viable parameter space are within the experimental limits.

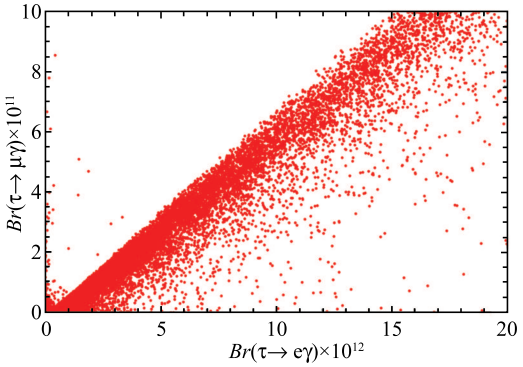

Fig. 5. Correlation plot between $Br(\tau \to e\gamma)$ and $Br(\tau \to \mu\gamma)$

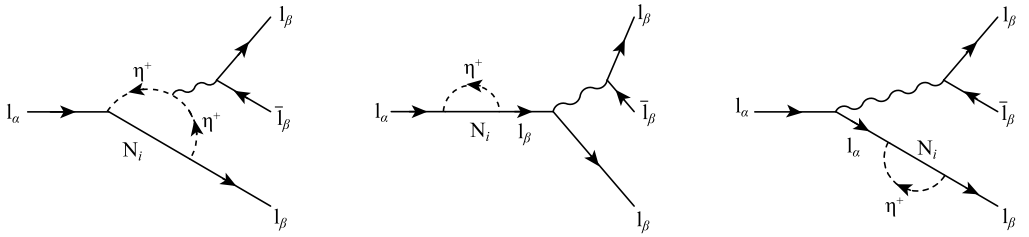

Fig. 6. Penguin diagram contributions to $l_\alpha \to 3l_\beta$. The mediator (wavy line) denotes either a photon or a Z-boson.

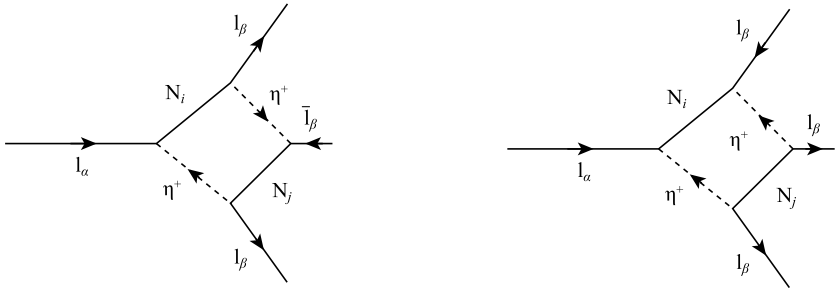

Fig. 7. Box diagram contributions to $l_\alpha \to 3l_\beta$.

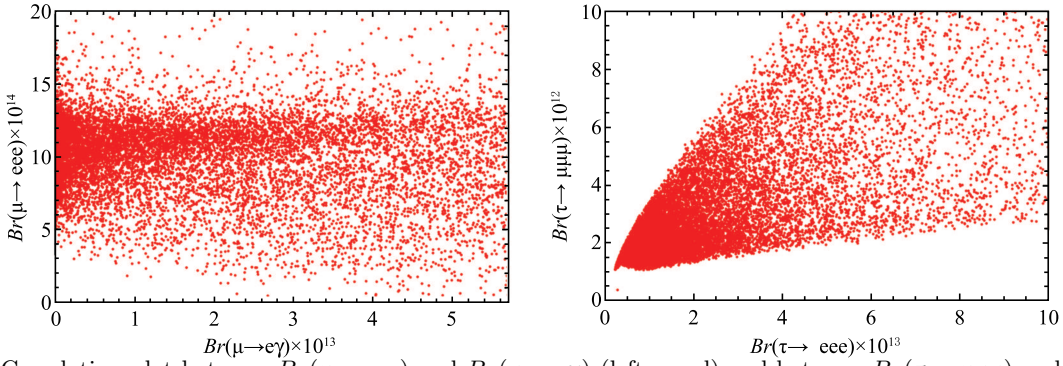

Fig. 8. Correlation plot between $Br(\mu \to eee)$ and $Br(\mu \to e\gamma)$ (left panel) and between $Br(\tau \to \mu\mu\mu)$ and $Br(\tau \to eee)$ (right panel).

6 Summary and conclusion

In this paper we have considered the scotogenic model, which is an extension of the Standard Model with an additional inert scalar doublet and three heavy Majorana right-handed neutrinos. It is a novel scenario connecting neutrino physics and dark matter. We have diagonalized the neutrino radiative mass matrix using the TBM matrix with an additional perturbed matrix as a rotation matrix in the 13 plane. The mixing angles are chosen ($\theta = 35^\circ$ and $\varphi = 12^\circ$) to accommodate a sizeable θ_{13}. Working in a degenerate heavy neutrino mass spectrum, we have obtained a flavor structure favourable to explain normal neutrino mass ordering. Choosing the lightest of the odd particles as dark matter, we have computed the relic abundance including the coannihilation effects. Scanning over the entire parameter space and applying the constraints from neutrino oscillation data, dark matter observables and bounds from lepton flavor violating decays such as $l_\alpha \to l_\beta\gamma$ and $l_\alpha \to 3l_\beta$, we have shown the suitable range for various parameters in the model.

Appendix A

Loop functions

The loop functions used in LFV decays are given by

$$F_2(x) = \frac{1-6x^2+3x^4+2x^6-6x^4\log x^2}{6(1-x^2)^4}, \tag{A1}$$

$$G_2(x) = \frac{2-9x^2+18x^4-11x^6+6x^6\log x^2}{6(1-x^2)^4}, \tag{A2}$$

$$D_1(x,y) = -\frac{1}{(1-x^2)(1-y^2)} - \frac{x^4\log x^2}{(1-x^2)^2(x^2-y^2)} - \frac{y^4\log y^2}{(1-y^2)^2(y^2-x^2)}, \tag{A3}$$

$$D_2(x,y) = -\frac{1}{(1-x^2)(1-y^2)} - \frac{x^2\log x^2}{(1-x^2)^2(x^2-y^2)} - \frac{y^2\log y^2}{(1-y^2)^2(y^2-x^2)}. \tag{A4}$$

In the limit $y \to x$, the functions D_1 and D_2 become

$$D_1(x,x) = \frac{-1+x^4-2x^2\log x^2}{(1-x^2)^3}, \tag{A5}$$

$$D_2(x,x) = \frac{-2+2x^2-(1+x^2)\log x^2}{(1-x^2)^3}. \tag{A6}$$

References

1 P. Minkowski, Phys. Lett. B, **67**: 421 (1977); R. N. Mohapatra and G. Senjanovic, Phys. Rev. Lett., **44**: 912 (1980); M. Gell-Mann, P. Ramond, and R. Slansky (1980), print-80-0576 (CERN); J. Schechter and J. W. F. Valle, Phys. Rev. D, **22**: 2227 (1980)

2 R. N. Mohapatra and G. Senjanovic, Phys. Rev. D, **23**: 165 (1981); G. Lazarides, Q. Shafi, and C. Wetterich, Nucl. Phys. B, **181**: 287 (1981); C. Wetterich, Nucl. Phys. B, **187**: 343 (1981); B. Brahmachari and R. N. Mohapatra, Phys. Rev. D, **58**: 015001 (1998); S. Antusch and S. F. King, Phys. Lett. B, **597**: 199 (2004); R. N. Mohapatra, Nucl. Phys. Proc. suppl., **138**: 257 (2005)

3 R. Foot, H. Lew, X. G. He et al, Z. Phys. C, **44**: 441 (1989)

4 E. Ma, Phys. Rev. D, **73**: 077301 (2006), arXiv:hep-ph/0601225

5 B. Pontecorvo, Sov. Phys. JETP, **7**: 172 (1958); Z. Maki, M. Nakagawa, and S. Sakata, Prog. Theor. Phys., **28**: 870 (1962)

6 F. P. An et al (DAYA-BAY Collaboration), Phys. Rev. Lett., **108**: 171803 (2012), arXiv:1203.1669

7 F. P. An et al (DAYA-BAY Collaboration), Chin. Phys. C, **37**: 011001 (2013), arXiv:1210.6327

8 J. K. Ahn et al (RENO Collaboration), Phys. Rev. Lett., **108**: 191802 (2012), arXiv:1204.0626

9 K. Abe et al (T2K Collaboration), Phys. Rev. D, **88**: 032002 (2013), arXiv:1304.0841

10 D. Forero, M. Tortela, and J. Valle, Phys. Rev. D, **90**: 093006 (2014), arXiv:1405.7540

11 P. A. R. Ade et al (Planck Collaboration), Astron. Astrophys., **571**: A1 (2014), arXiv:1303.5062

12 L. Lepoz Honorez, E.Nezri, J. F. Oliver et al, JCAP, **02**: 28 (2007), arXiv:hep-ph/0612275

13 R. Barbieri, L. E. Hall, and V. S. Rychkov, Phys. Rev. D, **74**: 015007 (2006), arXiv:hep-ph/0603188

14 M. Gustafsson, PoS CHARGED, **2010**: 030 (2010), arXiv:1106.1719

15 Daijiro Suematsu, Takashi Toma, Tetsuro Yoshida, Phys. Rev. D, **79**: 093004 (2009), arXiv:0903.0287

16 D. Schmidt, T Schwetz, and T. Toma, Phys. Rev. D, **85**: 073009 (2012), arXiv:1201.0906

17 T. Toma and A. Vicente, JHEP, **01**: 160 (2014), arXiv:1312.2840

18 A. Vicente, C E. Yaguna, JHEP, **02**: 144 (2015), arXiv:1412.2545

19 G. Altarelli, F. Ferugilo, Rev. Mod. Phys., **82**: 2701 (2010); G. Altarelli, F. Ferugilo, L. Merlo, and E. Stamou, JHEP, **08**: 021 (2012), arXiv:1205.4670; S. F. King and C. Luhn, Rept. Prog. Phys., **76**: 056201 (2013), arXiv:1301.1340; S. F. King, A. Merle, S. Morisi et al, New Journ. Phys., **16**: 045018 (2014); H. Isimori et al, Prog. Theor. Phys. Suppl., **183**: 1 (2010)

20 P. F. Harrison, D. H. Perkins, and W.G. Scott, Phys. Lett. B, **458**: 79 (1999); Phys. Lett. B, **530**: 167 (2002); Z. Z. Xing, Phys. Lett. B, **533**: 85 (2002); P. F. Harrison and W. G. Scott, Phys. Lett. B, **535**: 163 (2002); Phys. Lett. B, **557**: 76 (2003); X.-G. He and A. Zee, Phys. Lett. B, **560**: 87 (2003); L. Wolfenstein, Phys. Rev. D, **18**: 958 (1978); Y. Yamanaka, H. Sugawara, and S. Pakvasa, Phys. Rev. D, **25**: 1895 (1982); D, **29**: 2135(E) (1984); N. Li and B.-Q. Ma, Phys. Rev. D, **71**: 017302 (2005), arXiv:hep-ph/0412126

21 M. Sruthilaya, C. Soumya, K.N. Deepthi et al, New J. Phys., **17**: 083028 (2015), arXiv:1408.4392

22 K. Griest and D. Seckel, Phys. Rev. D, **43**: 3191 (1991)

23 K. A. Olive et al, Particle Data Group Collaboration, Chin. Phys. C, **38**: 090001 (2014)